Noname manuscript No.
(will be inserted by the editor)

Foot-Ground Contact Modeling within Human Gait Simulations: from Kelvin-Voigt to Hyper-Volumetric Models

Mohammad S. Shourijeh* · John McPhee

Received: date / Accepted: date

Abstract This study describes the development of a multibody foot-ground contact model consisting of spherical volumetric models for the surfaces of the foot. The developed model is two-dimensional and consists of two segments, the hind-foot, mid-foot, and fore-foot as one rigid body and the phalanges collectively as the second rigid body. The model has four degrees of freedom: ankle x and y, foot orientation, and metatarsal-phalangeal joint angle. Three different types of contact elements are targeted: Kelvin-Voigt, linear volumetric, and hyper-volumetric. The models are kinematically driven at the ankle and the metatarsal joints, and simulated horizontal and vertical ground reaction forces as well as center of pressure location are compared against experimental quantities, acquired from barefoot measurements during a human gait cycle. Parameter identification is performed for finding optimal contact parameters and locations of the contact elements. The hyper-volumetric foot-ground contact model was found to be a suitable choice for foot/ground interaction modeling within human gait simulations; this model showed 75% and 62% improvement on the matching quality over the point contact and linear volumetric models, respectively.

Keywords Foot-ground contact · Volumetric contact modeling · Gait

1 Introduction

Foot-ground contact modeling is an essential piece in predictive forward dynamic gait simulations. Contact forces affect the muscle, ligament, and joint reaction forces. Therefore, it plays a crucial role in understanding gait simulations, injury biomechanics, and design of prosthetics [7,22,27,29,38–40].

*Corresponding author:
Mohammad S. Shourijeh, Department of Systems Design Engineering, University of Waterloo, 200 University Avenue West, Waterloo, Ontario N2L 3G1, Canada
E-mail: msharifs@uwaterloo.ca

Many studies have included foot-ground contact models in human gait simulations; however, they lack either computational efficiency or accuracy in reproducing the ground reaction forces. Most previous studies have modeled the foot-ground interaction by means of kinematic constraints either hard or soft (spring-damper for the normal force) [2,8–11,14,21,31,36,37]. The point contact elements result in sharp contact forces that lead to inadequate reproduction of ground reaction forces (GRFs). For instance, [22,37] predicted ground reaction forces that do not match the measured quantities well. Also in [2,11,22], high frequency oscillations are reported at initial contact instants. One might circumvent this issue by increasing the number of contact elements as in [21,26], but this results in longer simulation time. Also, the more the number of contact elements, the more the number of parameters, and therefore the more challenging and computationally expensive the parameter identification will be. Some of the constraint-based contact models with single contact points, such as [8,14], require the constraint to act at the center of pressure (CoP), which will not help in predictive forward dynamic simulations for which no information of the CoP location is available.

On the other hand, there are models that are not based on point contact nodes but on contact patches. These models that integrate the pressure based on the normal deformation over the contact area are called volumetric models. This concept has been used to model the foot-ground interaction by spherical ([6] and Sec. 4.4 of [20]), cylindrical ([17,35]), and elliptical ([18,25]) elements. These volumetric contact elements are claimed to be more efficient than point contact nodes during simulations (nearly 18% faster and approximately 37% numerically less stiff); see Ch. 6 of Lopes [18]. Although Lopes presented promising GRF results using superellipsoids within a gait simulation, due to changes in the kinematics of the gait model during forward dynamics (like in [11]), the accuracy of the contact model cannot be assessed. Unfortunately, GRFs are not reported in either of [17,35], and therefore cannot be evaluated. The model presented in Sec. 4.4 of [20] consists of two segments with three spheres where the metatarsal-phalangeal (MP) joint was assumed to be a passive joint with a rotational spring and damper. A volumetric foot-ground contact model was based on the work by [12], which assumes a linear elastic foundation, i.e. small deformations. Although Güler et al. [6] were able to model the heel pad within impact tests of Valiant [33] using a linear foundation assumption reasonably well, this assumption does not seem well-suited for modeling of the contact element during gait. The heel pad soft tissue undergoes a significantly large deformation (in contrast with small deformations in the linear foundation models) in impact with the ground, which is reported to be up to 12 mm for a subject with 22.8 mm heel pad thickness (see Sec. 4.4 of [20]). As a result, the ground reaction forces of gait simulation reported by Güler et al.[6] did not sufficiently match the experimental data. It should be noted that Refs. [32,34] modeled the spherical contact elements using Hertz theory for the normal contact force, in which the normal force is calculated based on depth of deformation rather than deformed volume of the spheres, and therefore that approach is similar to point contact modeling. Although

they were able to make improvements on replicating the double hump of the experimental vertical GRF, the transition between their four spheres was not smooth due to the contact formulation or locations of those spheres.

This research studies the development of a two-dimensional multibody foot-ground contact model consisting of spherical geometries for the foot surfaces representing the heel, metatarsal joints, and toes. The nonlinear volumetric foot-ground contact model is expected to provide higher fidelity than the point contact models as volumetric elements provide a wider contact area, and therefore smoother contact forces. This model is expected to produce better results than the one in Sec. 4.5 of [20] as the MP joint is driven kinematically, separately from the ankle, to provide more consistency and accuracy at toe-off. More importantly, the volumetric model is improved using the concept of hyper-elastic material foundation based on Sec. 3.2 of [23]; additionally, the developed model includes linear dampers to account for impact velocity dependency of the foot pad material and also energy dissipation as reported by [1,20].

A preliminary version of this work has been reported previously [28], and permission for publishing some of the text and figures has been granted by American Society of Mechanical Engineers.

2 Model

In this section, first the geometry of the foot is discussed. Later, three different contact scenarios for modeling the normal force are presented, and at the end a friction model is introduced.

2.1 Foot geometry

The model is two dimensional with two rigid body segments: the hind-foot, mid-foot, and fore-foot as one rigid body and the phalanges collectively as the second rigid body. The model has four degrees of freedom: ankle positions x_A and y_A, foot orientation θ_F, and MP joint angle ϕ_P. Both ankle and MP joints are assumed to be revolute joints.

The parametric foot model is depicted in Fig. 1. Points A, H, P, and T approximately represent the ankle, heel, 1st MP joint, and toe tip, respectively. The lengths in this model were measured from the subject on which the experiment was performed; however, to have the best foot geometry compatible with the marker positions, a geometry fitting procedure is carried out that is explained in detail later on.

Three types of contact models are detailed in the coming sections. Note that the initial locations of contact elements are at the characteristic points H, P, and T, which is a restricting assumption. To remove this restriction, the positions of the contact elements are relaxed within a certain range. For this goal, the location of the elements are allowed to move slightly in both local

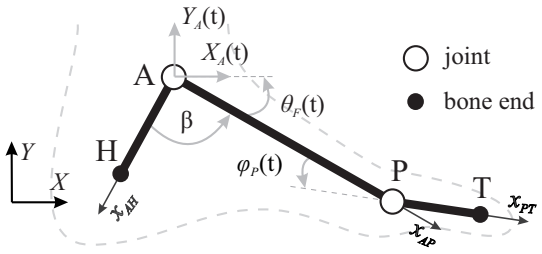

Fig. 1: Parametric foot geometry

x and y directions (as shown in Fig. 1) so that the elements are posed at the optimal locations H*, P*, and T*.

2.2 Nonlinear spring-linear damper contact model

The general point contact force can be written as:

$$f_n = K(\delta) + D(\dot{\delta}) \tag{1}$$

which includes a stiffness term as a nonlinear function of spring deformation δ and a damping term as a function of the rate of deformation $\dot{\delta}$. However, this shape of the contact function will result in a spiky contact force at the initial contact instant. The formulation applied here is based on the model proposed by Hunt and Crossley [16], which inhibits the contact element from undergoing a drastic force change at the initial impact due to the velocity of the contact point.

$$f_n = \begin{cases} k_S \mid L - L_0 \mid^{n_S} (1 + a_S v_n) & L \leq L_0 \\ 0 & otherwise \end{cases} \tag{2}$$

where k_S and a_S are the spring stiffness and pseudo-damping, respectively, L_0 is the rest length, and n_S is the nonlinearity exponent, which form the set of four parameters of this contact model. The variable L is the spring length and v_n is the vertical velocity of the contact point.

2.3 Linear volumetric contact model

Kelvin-Voigt elements are replaced with spheres, as shown in Fig. 2, to supply wider contact areas and therefore produce smoother normal contact forces. The contact model is based on a volumetric approach [4,12]. This model assumes a linear elastic foundation for the material. Millard 2011 (Ch. 4 of [20]) did some in-vivo measurements of the heel pad deformation and force, and they concluded that the volumetric contact could be a suitable candidate for human foot-ground contact modeling.

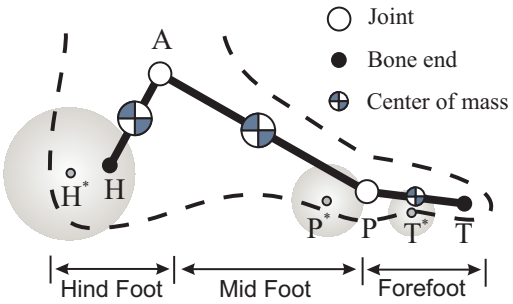

Fig. 2: Schematic foot with three spherical volumetric contact elements. H*, P*, and T* are the relaxed locations of the contact spheres.

The idea, instead of using a point contact as in the previous model, assumes a linear pressure distribution $p(s)$, which is a function of the location s on the contact patch $\mathbf{S}$, as shown in Fig. 3. Consider the schematic representation of a sphere interacting with the ground. The body $\mathbf{B}_i$ is the deformable body (foot), whereas $\mathbf{B}_j$ is the rigid and fixed body (ground). Therefore the interpenetration volume V is written as:

$$V = \int_S \delta(s) dS = \int_V dV \tag{3}$$

where δ is the deformation at location s. The pressure distribution is defined using the theory proposed by Hunt and Crossley [16] as below:

$$p(s) = k_V \delta(s)(1 + a_V \dot{\delta}(s)) \tag{4}$$

where k_V and a_V are stiffness and pseudo-damping of the foundation, respectively, and $\dot{\delta}(s)$ is the rate of deformation at point s. Then the total normal contact force will be given by:

$$f_n = \int_S p(s) dS \tag{5}$$

which can be written in the form of a vector function of the deformed volume as:

$$\mathbf{f_n} = k_V V(1 + a_V v_{cn})\hat{\mathbf{n}} \tag{6}$$

where $\mathbf{f_n}$ is the normal force, V is the interpenetration volume, $\hat{\mathbf{n}}$ is the outward unit vector normal to S, and v_{cn} is the normal velocity at the center of mass of the deformed volume.

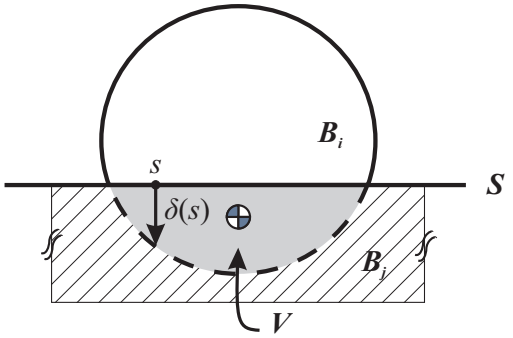

Fig. 3: Schematic of the volume of the interpenetration between two bodies in contact

2.4 Nonlinear volumetric contact model

The principal shortcoming of the previous model is the linearity assumption in the material model. Gonthier et al. [13] assumed a linear elastic foundation model, which is suitable for small deformation ranges, as they initiated the technique for metal on metal contact; however, the soft heel tissue undergoes a maximum deformation of 53.6% reported by Millard 2011 (Ch. 4 of [20]) considering a 22.8 mm thickness for the heel pad and 12 mm of the maximum deformation. Therefore, the linear foundation assumption is likely not valid for a foot. Alternatively, the foundation can be modeled as a hyper-elastic material, see Sec. 3.2 of [23].

Consider a hyper-elastic foundation with no damping. The normal force can be written as:

$$\mathbf{f_n} = (k_V V_h)\hat{\mathbf{n}} \tag{7}$$

where the hypervolume V_h is expressed as the following:

$$V_h = \iint_S \delta^\eta(s)\ dS = c_v(V) \iint_S \delta(s)\ dS = c_v(V)V \tag{8}$$

with

$$c_v(V) = \frac{\iint_S \delta^\eta(s)\ dS}{\iint_S \delta(s)\ dS}$$

It was shown in [23] that the hypervolume V_h is a linear function of the penetration volume V in a double logarithmic scale. Therefore the hypervolume coefficient $c_v(V)$ can be written as:

$$c_v(V) = e^{a_0 + a_1 \ln(V)} \tag{9}$$

where a_0 and a_1 are parameters that depend on the foundation nonlinearity η and geometrical properties. In other words, for a given contact geometry and hyper-elasticity exponent, there exist unique values for a_0 and a_1. Therefore, the normal force can be written as:

$$\mathbf{f_n} = (k_V c_v(V)\ V)\hat{\mathbf{n}} = (k_V e^{a_0 + a_1 \ln(V)}\ V)\hat{\mathbf{n}} \tag{10}$$

For more details on this hyper-volumetric contact modeling approach, see Sec. 3.2 of [23] or [24].

Eq. 10 can be further simplified as:

$$\mathbf{f_n} = (k_h V^{\mathcal{H}})\hat{\mathbf{n}} \ \text{ where } \ k_h = k_V e^{a_0} \ \text{ and } \ \mathcal{H} = 1 + a_1 \tag{11}$$

The pressure distribution assumed for the hyper-elastic foundation in the foot, including damping, is the following:

$$p(s) = k_V \delta^{\eta}(s) + k_V \delta(s) a_V v_n \tag{12}$$

which implies that there is a nonlinear stiffness term, but the damping term is still linear. Then the normal force can be written as:

$$\mathbf{f_n} = (k_h V^{\mathcal{H}} + a_h V v_{cn})\hat{\mathbf{n}} \tag{13}$$

where k_h, which is called a nonlinear volumetric pseudo-stiffness here, and exponent $\mathcal{H}$ depend on both the volumetric stiffness and geometrical properties; a_h is the foundation stiffness k_V multiplied by the damping a_V as in the linear volumetric formulation.

2.5 Friction model

An approximation of the dry Coulomb model is used to compute the force of friction between the contact spheres in the foot model and the ground:

$$f_f = -\mu(v_{ct}) f_n \tag{14}$$

where f_f is the friction force for the sphere, v_{ct} is the tangential speed of the centroid of the deformed volume, and $\mu(v_{ct})$, shown in Fig. 4, is the friction coefficient function defined to guarantee the differentiability of the expression as follows:

$$\mu(v_{ct}) = \mu_f \arctan(v_{ct}/v_s) \tag{15}$$

where μ_f is the asymptotic friction coefficient and v_s is a shape parameter. The smaller the shape factor v_s, the closer the approximation to the dry Coulomb friction.

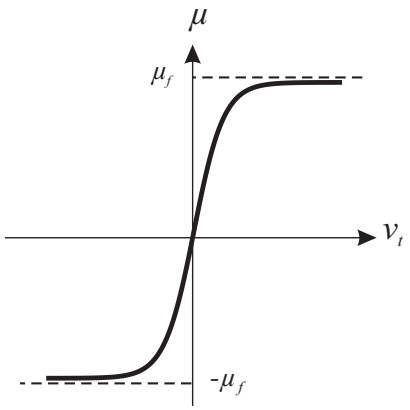

Fig. 4: Plot of the friction coefficient function versus tangential speed

3 Methods

3.1 Experimental data

Data from one healthy active male (age 23; weights 79 kg; height 1.76) was used in this study. Barefoot subject was asked to walk at his preferred speed while his right foot stepping on a Bertec force platform, which was used to capture grounds reaction forces.

Nine Vicon cameras measured locations of six markers mounted on medial and lateral malleolus, posterior calcaneous, the first and the fifth MP joints, and nail of the first toe. Triggered data collection of kinematics, and GRFs was repeated three times, but only one arbitrary trial was used here. GRFs and kinematics were sampled at 1000 Hz and 200 Hz, respectively, and they were filtered by a 4th order Butterworth dual low-pass filter with cut-off frequency of 20 Hz [3].

3.2 Geometry fitting

The parameterized foot was driven at all four degrees of freedom to produce a set of kinematics as close as possible to the experimental marker positions within an iterated optimization procedure. x_A, y_A and foot orientation θ_F were taken from the processed kinematic data, but the MP joint angle was parameterized with an 11-term Fourier series as in Eqn. 16. This implies that the experimental kinematics should be considered in one period of motion (0.97 s), from one toe-off to the next toe-off. The Fourier series functions are suitable choices for joint angles ([22]), muscle excitations ([30]), and muscle forces ([29]) in periodic motions. The coefficients of these functions are treated as parameters in the identification process, which is a typical method in converting an

optimal control problem to a parameterized optimization.

$$\phi_P(t) = A_0 + \sum_{k=1}^{5}[A_k \sin(\frac{2\pi kt}{T}) + B_k \cos(\frac{2\pi kt}{T})] \tag{16}$$

The parameters to be identified are lengths AH, AP and PT, angle β, and coefficients of the Fourier series representing MP joint angle, resulting in a total of 15 parameters. Parameter identification is done in MATLAB® [19] using a combination of a genetic algorithm, a pattern search, and a sequential quadratic programming algorithm. Details on the optimization and convergence study are described later in Sec. 3.3.

3.3 Contact model Identification

Three different contact models were investigated: nonlinear spring and linear damper, linear volumetric sphere, and a nonlinear volumetric sphere. In a foot model, one element of each type is employed at points H, P, and T. For each case, the model is kinematically driven at the ankle and metatarsal joints using the experimental position at the ankle and hind-foot orientation data, and the identified angle at the MP joint. Parameters of each model are then iterated within an optimization procedure so that the generated vertical and friction forces and the center of pressure position computed by the model match the experimental data as close as possible. The objective function to be minimized, of matching non-dimensionalized criteria with equal weighting, is written as:

$$J = \frac{1}{T}\int_0^T \left\{ \left[\frac{f_n^m - f_n^e}{\sigma(f_n^e)}\right]^2 + \left[\frac{f_f^m - f_f^e}{\sigma(f_f^e)}\right]^2 + \left[\frac{X_{Cop}^m - X_{Cop}^e}{\sigma(X_{Cop}^e)}\right]^2 \right\} dt \tag{17}$$

where J designates the objective function, T is the gait cycle period, f_n is normal force, f_f is friction force, and X_{Cop} represents the location of the center of pressure. σ is the standard deviation, and superscripts m and e correspond to model and experiment, respectively.

For the convergence study for each case, three different random initial points were obtained by solving the optimization problem running a genetic algorithm (GA) in MATLAB® [19] for a maximum of 100 populations. Afterwards, these three solutions were used to run a sequential quadratic programming (SQP) solver to take advantage of faster gradient-based algorithms. From those three runs, the best one was chosen to be the raw optimum. Using this new solution as a new initial guess, the Pattern Search (PS) function as a direct search routine was then run. If the objective function value of the PS was less, it was put into the SQP again. This cycle was repeated until the change in the values of the objective function and bound violations were less than 1e-6, where the result was accepted as the final optimum.

4 Results

Geometrical parameters of the best fitted geometry that could follow the experimental marker positions are shown in Tab. 1. The lengths AH, AP and PT were in good agreement with the lengths measured on the subject. The kinematic model and simulation of the foot reproduced the experimentally recorded marker positions with an error of 3.7±4.3 mm.

Table 1: Optimal parameters of the foot geometry consistent with the marker data

Parameter	Optimal Value
AH (cm)	8.2
AP (cm)	15.4
PT (cm)	6.9
β (deg)	108

In Fig. 5, the results of all three contact models are plotted against experimental data: point contact model (a,d,g), linear volumetric model (b,e,h), and hyper-volumetric model (c,f,i). The first row in Fig. 5 depicts the normal contact forces, whereas the second and third rows show the friction forces and CoP locations, respectively.

The bounds on the parameters and the optimal values acquired from parameter identification for spring-damper, linear volumetric, and hyper-volumetric models are presented in Tables 2, 3, and 4 in Appendix A, respectively.

The objective function value for the point contact model was 0.69, whereas this value was 0.44 and 0.17 for linear volumetric and hyper-volumetric models, respectively.

5 Discussion

By looking at Fig. 5a, it is observed that the point contact model is not a good representation of human foot-ground contact during gait. As can be seen, there is not a smooth transition between peaks present in the contact force. Furthermore, these spikes in the normal force are reflected in the friction force (Fig. 5d) as well. Note that the friction force is also affected by speed variations at the contact point. The objective function (based on Eqn. 17) value attained for this model was 0.69. There are at least two options to improve the results: modifying the contact model, or increasing the number of contact elements as in [11,21]. Modification of the contact model is chosen here.

As depicted in Fig. 5b, the normal contact force from the linear volumetric model is much closer to the experimental value than the one shown in Fig. 5a, which can also be elicited by comparing the friction forces (Fig. 5e to Fig. 5d).

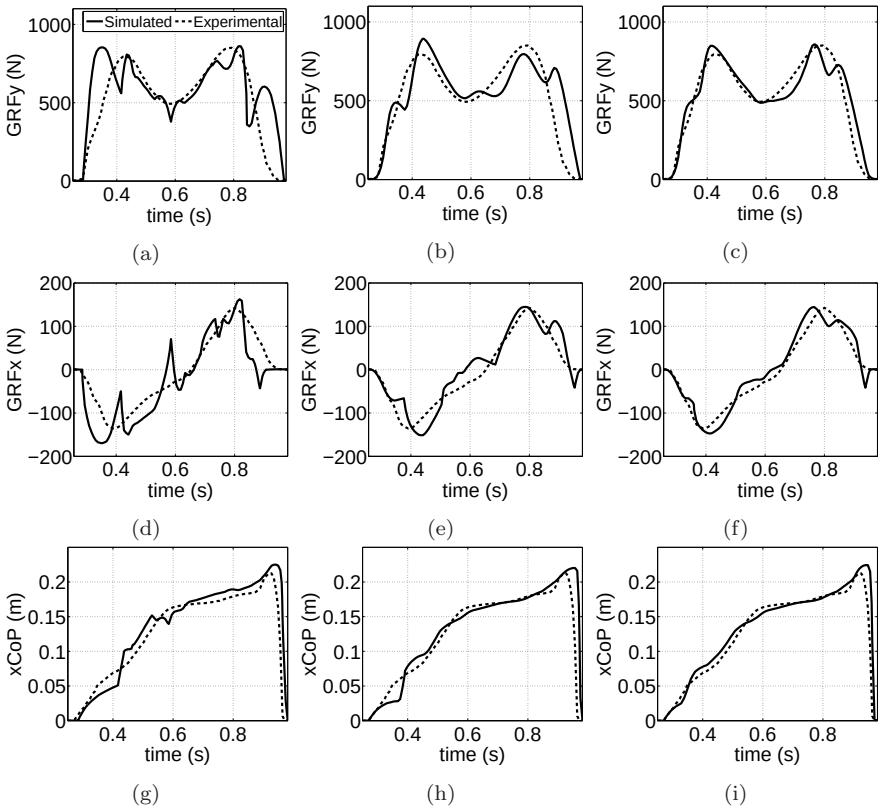

Fig. 5: Results of the spring-damper contact model (a,d,g), linear volumetric model (b,e,h), and hyper-volumetric model (c,f,i). The first row in each column is the vertical force, the second row is the horizontal force, and the third row shows the location of the center of pressure. In all plots, the dashed line is the experimentally measured data whereas the solid line is the simulated quantity.

The corresponding objective function for the linear volumetric model is 0.44, which implies a 36% decrease in calibration error, and therefore a significant improvement in the contact model over the Kelvin-Voigt model. However, the results are not fully satisfying as oscillatory behavior is still observed in the contact force. This can be related to lack of fidelity of the contact model, the low number of contact spheres, or due to errors in the kinematic data. Our focus in this study is on modifying the contact model.

The last phase of model modification in this study is devoted to replacing linear volumetric spheres with nonlinear volumetric elements. The optimal parameter values of this model are presented in Table 4 in Appendix A. The results of the hyper-volumetric model are depicted in Figs. 5(c,f,i) and the optimal parameters for the three spheres of this model are listed in Table 4 (Appendix A). The normal contact force is smoother than that of the linear

volumetric model, which implies that a nonlinear model is a more accurate representation of the foot/ground interaction. Additionally, the quality of the friction force (Fig. 5f) reveals preference of the hyper-volumetric model over the other two. We believe that there is obvious room for improvement of the friction model. It should be noted that there were only two parameters in the tangential force model for Coulomb friction. Despite that, by looking at the simulated and experimental tangential ground reaction forces, a reasonable match can be interpreted. The comparison of the center of pressure position with the experimental CoP also reveals a quite reasonable match. The value of J for this model was 0.17, which implies 62% and 75% decrease in the objective function over the linear volumetric and Kelvin-Voigt models, respectively.

The positions of the contact elements were relaxed within a certain range (unlike [28]), which had been also done in previous studies, such as [32,34]. This can be justified as to account for "skin stretch" during gait ([15], Ch. 4 of [20]). Although relaxing the contact locations results in a total of 6 more parameters, it provides better estimates of the locations of contact elements, and consequently more reasonable and smoother contact forces.

Although the volumetric approach was previously utilized by [20] for foot-ground contact modeling, this current study had significant differences: the MP joint was driven with independent kinematics to provide a smoother transition at toe-off, the volumetric contact model used in this study was nonlinear, and the locations of spheres were identified by optimization. These changes improved the contact forces significantly.

Additionally, the proposed hyper-volumetric model had a different concept than that presented by Sandhu and McPhee [25]. Their model was nonlinear, but they did not compute any closed-form volumes; they computed the deformed volumes numerically, which leads to slower simulations. In other words, they discretized the foundation to finite Kelvin-Voigt elements, and then calculated the contact forces by adding the forces of those elements, which is more similar to the study by Gilchrist and Winter [11] than a volumetric approach.

The foot model in this study was two dimensional (2D), and can only be used in 2D gait simulations. It must be noted that human gait is a 3D movement, and the rotations in the frontal plane are disregarded once 2D models are used. This plays an important role in the foot-ground contact modeling due to considerable inversion/eversion of the foot during the stance phase [5], which may prevent model from producing a perfect match to the data that are actually coming from a 3D motion. Therefore, for more fidelity, foot-ground interactions should be modeled in 3D, and the GRF of the third direction as well as the motion of the CoP in that direction must be taken into account.

6 Conclusions and future work

A dynamic foot model was developed and calibrated within a gait simulation. Three different types of contact scenarios were modeled: point contact, linear

volumetric, and nonlinear volumetric. The transition from a point contact to a volumetric model showed a promising progress in generating the contact force in agreement with the experimental data. For the nonlinear volumetric model, the vertical and horizontal ground reaction forces and the center of pressure of the nonlinear volumetric foot-ground contact model showed excellent correlations with the experimental data. This means that a nonlinear volumetric contact element is a suitable choice for human foot-ground contact modeling.

Although the spherical volumetric elements produced reasonable results, which were much better than the point contact models as they provide a wider contact patch, more complicated shapes like an ellipsoid as in [25] and Ch. 6 of [18] can be employed in the future.

The contact model was a sphere on surface, which is three-dimensional per se; however, the forces of the third dimension were not validated. Thus, in the future, it would be interesting to study the friction forces of the lateral direction to compare the simulated and experimental quantities of this force as well, for which the foot model must be three-dimensional as well.

More sets of experimental data will be required to fully validate the foot-ground contact model. In other words, provided different experimental conditions like slow and fast walking, jogging, and running, and also with different footwear conditions, the model can be validated in a more general and therefore robust way.

A more complicated friction model such as the bristle model proposed by Gonthier et al. [13] can replace the Coulomb friction model. There is an obvious room for improving the friction model by looking at the simulated and experimental results.

Acknowledgements We thank Mr. Michael Boos for providing us with the linear volumetric contact components in MapleSim. We also wish to thank the Human Movement Biomechanics Lab at the University of Ottawa for assistance with the data collection. The first author would like to thank Dr. Willem Petersen for the helpful discussion of the hypervolumetric contact modeling approach. The authors also wish to acknowledge the Natural Sciences and Engineering Research Council of Canada (NSERC) for funding support of this study.

References

1. Aerts, P., Ker, R.F., De Clercq, D., Ilsley, D.W., Alexander, R.M.: The mechanical properties of the human heel pad: A paradox resolved. Journal of Biomechanics **28**(11), 1299–1308 (1995)
2. Anderson, F.C., Pandy, M.G.: Dynamic optimization of human walking. Journal of Biomechanical Engineering **123**(5), 381–390 (2001)
3. Bisseling, R.W., Hof, A.L.: Handling of impact forces in inverse dynamics. Journal of Biomechanics **39**(13), 2438 – 2444 (2006)
4. Boos, M., McPhee, J.: Volumetric modeling and experimental validation of normal contact dynamic forces. Journal of Computational and Nonlinear Dynamics **8**(2), 021,006 (2013)
5. Carson, M., Harrington, M., Thompson, N., O'Connor, J., Theologis, T.: Kinematic analysis of a multi-segment foot model for research and clinical applications: a repeatability analysis. Journal of Biomechanics **34**, 1299–1307 (2001)

6. Cenk Güler, H., Berme, N., Simon, S.R.: A viscoelastic sphere model for the representation of plantar soft tissue during simulations. Journal of biomechanics **31**(9), 847–853 (1998)
7. Cole, G.K., Nigg, B.M., van den Bogert, A.J., Gerritsen, K.G.M.: Lower extremity joint loading during impact in running. Clinical Biomechanics **11**(4), 181–193 (1996)
8. Dorn, T.W., Lin, Y.C., Pandy, M.G.: Estimates of muscle function in human gait depend on how foot-ground contact is modelled. Computer methods in biomechanics and biomedical engineering **15**(6), 657–668 (2012)
9. Erdemir, A., Piazza, S.J.: Changes in foot loading following plantar fasciotomy: A computer modeling study. Journal of Biomechanical Engineering **126**(2), 237–243 (2004)
10. Geyer, H., Herr, H.: A muscle-reflex model that encodes principles of legged mechanics produces human walking dynamics and muscle activities. Neural Systems and Rehabilitation Engineering, IEEE Transactions on **18**(3), 263–273 (2010)
11. Gilchrist, L.A., Winter, D.A.: A two-part, viscoelastic foot model for use in gait simulations. Journal of Biomechanics **29**(6), 795–798 (1996)
12. Gonthier, Y., McPhee, J., Lange, C., Piedboeuf, J.C.: A contact modeling method based on volumetric properties. In: ASME Conference Proceedings, vol. 2005, pp. 477–486
13. Gonthier, Y., McPhee, J., Lange, C., Piedbuf, J.C.: A regularized contact model with asymmetric damping and dwell-time dependent friction. Multibody System Dynamics **11**(3), 209–233 (2004)
14. Hamner, S.R., Seth, A., Steele, K.M., Delp, S.L.: A rolling constraint reproduces ground reaction forces and moments in dynamic simulations of walking, running, and crouch gait. Journal of biomechanics **46**(10), 1772–1776 (2013)
15. Holden, J.P., Orsini, J.A., Siegel, K.L., Kepple, T.M., Gerber, L.H., Stanhope, S.J.: Surface movement errors in shank kinematics and knee kinetics during gait. Gait & Posture **5**(3), 217–227 (1997)
16. Hunt, K., Crossley, F.: Coefficient of restitution interpreted as damping in vibroimpact. Journal of Applied Mechanics **7**, 440–445 (1975)
17. Kecskemethy, A.: Integrating efficient kinematics in biomechanics of human motions. Procedia IUTAM **2**, 86–92 (2011)
18. Lopes, D.S.: Smooth convex surfaces for modeling and simulating multibody systems with compliant contact elements. PhD Thesis, Instituto Superior Técnico, Universidade de Lisboa (2013)
19. MATLAB: version 8.0 (R2012b). The MathWorks Inc., Natick, Massachusetts, USA (2012)
20. Millard, M.: Mechanics and control of human balance. Ph.D. thesis, University of Waterloo, Canada (2011)
21. Neptune, R.R., Wright, I.C., Den Bogert, A.J.V.: A method for numerical simulation of single limb ground contact events: Application to heel-toe running. Computer Methods in Biomechanics and Biomedical Engineering **3**(4), 321–334 (2000)
22. Peasgood, M., Kubica, E., McPhee, J.: Stabilization of a dynamic walking gait simulation. Journal of Computational and Nonlinear Dynamics **2**(1), 65–72 (2007)
23. Petersen, W.: A volumetric contact model for planetary rover wheel/soil interaction. Ph.D. thesis, University of Waterloo, Canada (2012)
24. Petersen, W., McPhee, J.: A nonlinear volumetric contact model for planetary rover wheel/soil interaction. In: ASME International Design Engineering Technical Conferences, Portland, USA (2013)
25. Sandhu, S., McPhee, J.: A two-dimensional nonlinear volumetric foot contact model. In: ASME International Mechanical Engineering Congress & Exposition, Vancouver, Canada (2010)
26. Scott, S.H., Winter, D.A.: Biomechanical model of the human foot: kinematics and kinetics during the stance phase of walking. Journal of biomechanics **26**(9), 1091–1104 (1993)
27. Shourijeh, M.S.: Optimal control and multibody dynamic modelling of human musculoskeletal systems. PhD Thesis, University of Waterloo, Canada (2013)
28. Shourijeh, M.S., McPhee, J.: Efficient hyper-volumetric contact dynamic modelling of the foot within human gait simulations. In: ASME International Design Engineering Technical Conferences, Portland, USA (2013)

29. Shourijeh, M.S., McPhee, J.: Forward dynamic optimization of human gait simulations: A global parameterization approach. Journal of Computational and Nonlinear Dynamics **9**(3), 031,018 (2014)
30. Shourijeh, M.S., McPhee, J.: Optimal control and forward dynamics of human periodic motions using fourier series for muscle excitation patterns. Journal of Computational and Nonlinear Dynamics **9**(2), 021,005 (2014)
31. Srinivasan, S., Raptis, I., Westervelt, E.R.: Low-dimensional sagittal plane model of normal human walking. Journal of biomechanical engineering **130**(5), 051,017 (2008)
32. U. Lugris J. Carlin, R.P.V.J.L., J.Cuadrado: Solution methods for the double-support indeterminacy in human gait. Multibody System Dynamics **30**(3), 247–263 (2013)
33. Valiant, G.A.: A determination of the mechanical characteristics of the human heel pad in vivo. PhD Thesis, The Pennsylvania State University, USA (1984)
34. Vila, R.: Application of multibody dynamics techniques to the analysis of human gait. PhD Thesis, Technical University of Catalonia, Spain (2012)
35. Wang, J.M., Hamner, S.R., Delp, S.L., Koltun, V.: Optimizing locomotion controllers using biologically-based actuators and objectives. ACM Transactions on Graphics (TOG) **31**(4), 25 (2012)
36. Wilson, C., King, M.A., Yeadon, M.R.: Determination of subject-specific model parameters for visco-elastic elements. Journal of Biomechanics **39**(10), 1883–1890 (2006)
37. Wojtyra, M.: Multibody simulation model of human walking. Mechanics Based Design of Structures and Machines **31**(3), 357–379 (2003)
38. Zajac, F.E., Neptune, R.R., Kautz, S.A.: Biomechanics and muscle coordination of human walking, part i: Introduction to concepts, power transfer, dynamics and simulations. Gait & Posture **16**(3), 215–232 (2002)
39. Zajac, F.E., Neptune, R.R., Kautz, S.A.: Biomechanics and muscle coordination of human walking: Part ii: Lessons from dynamical simulations and clinical implications. Gait & Posture **17**(1), 1–17 (2003)
40. Zhou, X., Draganich, L.F., Amirouche, F.: A dynamic model for simulating a trip and fall during gait. Medical Engineering & Physics **24**(2), 121–127 (2002)

Nomenclature

δ	deformation
$\dot{\delta}$	rate of deformation
η	nonlinearity exponent of the foundation in the nonlinear volumetric contact model
$\mathcal{H}$	nonlinearity exponent of the volume in the nonlinear volumetric contact model
μ_f	friction asymptotic coefficient
ϕ_P	metatarsal-phalangeal joint angle
θ_F	foot orientation
a_h	pseudo-damping of the nonlinear volumetric model
A_i	coefficients of sin terms in Fourier series
a_S	pseudo-damping of the Kevin-Voigt model
a_V	volumetric pseudo-damping
B_i	coefficients of cos terms in Fourier series
D	damping
dx	relaxation parameter for characteristic points of the contact model in local x direction
dy	relaxation parameter for characteristic points of the contact model in local y direction

f_f	friction force
f_n	normal contact force
GRF_X	horizontal ground reaction force
GRF_Y	vertical ground reaction force
K	stiffness
k_h	pseudo-stiffness of the nonlinear volumetric model
k_S	spring stiffness
k_V	volumetric stiffness
L	spring length
L_0	spring rest length
n_S	nonlinearity exponent of the spring force-length relation
$p(s)$	foundation pressure distribution
R_V	radius of the contact element sphere
T	motion period
V_h	deformed hyper-volume
v_n	normal speed
v_s	shape parameter in the friction model
v_{cn}	normal speed of the centroid of the deformed volume
v_{ct}	tangential speed of the centroid of the deformed volume
X_{Cop}	center of pressure location

A Optimal Contact Parameters

Optimal parameters of the three different contact models are presented here.

Table 2: Optimal contact parameters of the spring-damper elements: k_S is the spring stiffness, a_S is the pseudo-damping, L_0 is the spring initial length, n_S is the non-linearity exponent, μ_f is the asymptotic friction coefficient, and v_s is a shape parameter for approximation of the dry Coulomb friction. Parameters dx and dy for characteristic points H, P, and T are expressed in local frames AH, AP, and PT, respectively.

Parameter	Spring	Optimal Value	Lower Bound	Upper Bound
k_S (N/m^n)	H	9.8e3	0	-
	P	2.2e3	0	-
	T	6.6e4	0	-
a_S (s/m)	H	85.7	0	-
	P	1.3e3	0	-
	T	15.8	0	-
L_0 (mm)	H	55	1	60
	P	50	1	55
	T	42	1	45
n_S	H	0.93	0.1	10
	P	0.95	0.1	10
	T	0.89	0.1	10
μ_f	H	0.33	1e-3	1
	P	0.41	1e-3	1
	T	0.45	1e-3	1
v_s (m/s)	H	0.062	1e-6	0.1
	P	0.035	1e-6	0.1
	T	0.055	1e-6	0.1
dx (mm)	H	-14.2	0	20
	P	-12.9	0	20
	T	-0.6	0	20
dy (mm)	H	-9.3	0	20
	P	8.4	0	20
	T	18.2	0	20

Table 3: Optimal contact parameters of the linear volumetric elements: k_V is the volumetric stiffness, a_V is the volumetric pseudo-damping, R_V is the radius of the sphere element, μ_f is the asymptotic friction coefficient, v_s is a shape parameter for approximation of the dry Coulomb friction, and dx and dy are local coordinates of the optimal positions of contact elements.

Parameter	Sphere	Optimal Value	Lower Bound	Upper Bound
k_V (N/m^3)	H	1.94e6	0	-
	P	2.08e6	0	-
	T	4.12e5	0	-
a_V (s/m)	H	1.6	0	-
	P	0.53	0	-
	T	0.31	0	-
R_V (mm)	H	56	1	60
	P	54	1	55
	T	43	1	45
μ_f	H	0.24	1e-3	1
	P	0.28	1e-3	1
	T	0.34	1e-3	1
v_s (m/s)	H	0.029	1e-6	0.1
	P	0.052	1e-6	0.1
	T	0.059	1e-6	0.1
dx (mm)	H	-11.9	0	20
	P	-13.4	0	20
	T	-0.8	0	20
dy (mm)	H	-10.8	0	20
	P	7.9	0	20
	T	17.8	0	20

Table 4: Optimal contact parameters of the nonlinear volumetric elements: k_h is the nonlinear volumetric pseudo-stiffness, a_h is the nonlinear volumetric pseudo-damping, R_V is the radius of the sphere element, $\mathcal{H}$ is the nonlinearity exponent of the volume, μ_f is the asymptotic friction coefficient, v_s is a shape parameter for approximation of the dry Coulomb friction, and dx and dy are local coordinates of the optimal positions of contact elements.

Parameter	Sphere	Optimal Value	Lower Bound	Upper Bound
k_h $(N/m^{3\mathcal{H}})$	H	7.4e5	0	-
	P	1.1e6	0	-
	T	6.8e5	0	-
a_h (Ns/m^4)	H	4.1e7	0	-
	P	6.3e5	0	-
	T	1.9e7	0	-
R_V (mm)	H	54	1	60
	P	52	1	55
	T	43	1	45
$\mathcal{H}$	H	0.78	0.1	10
	P	0.85	0.1	10
	T	0.83	0.1	10
μ_f	H	0.24	1e-3	1
	P	0.27	1e-3	1
	T	0.35	1e-3	1
v_s (m/s)	H	0.031	1e-6	0.1
	P	0.048	1e-6	0.1
	T	0.061	1e-6	0.1
dx (mm)	H	-12.0	0	20
	P	-13.1	0	20
	T	2.1	0	20
dy (mm)	H	-10.6	0	20
	P	8.3	0	20
	T	18.5	0	20